JACS
JOURNAL OF THE AMERICAN CHEMICAL SOCIETY

Communication

pubs.acs.org/JACS

Phosphine Quenching of Cyanine Dyes as a Versatile Tool for Fluorescence Microscopy

Joshua C. Vaughan,[†,‡] Graham T. Dempsey,[‡] Eileen Sun,[§] and Xiaowei Zhuang*[,†,‡,∥]

[†]Howard Hughes Medical Institute, [‡]Department of Chemistry and Chemical Biology, [∥]Department of Physics, Harvard University, Cambridge, Massachusetts, 02138, United States

[§]Graduate Program in Virology, Harvard Medical School, Boston, Massachusetts, 02115, United States

Supporting Information

ABSTRACT: We report that the cyanine dye Cy5 and several of its structural relatives are reversibly quenched by the phosphine tris(2-carboxyethyl)phosphine (TCEP). Using Cy5 as a model, we show that the quenching reaction occurs by 1,4-addition of the phosphine to the polymethine bridge of Cy5 to form a covalent adduct. Illumination with UV light dissociates the adduct and returns the dye to the fluorescent state. We demonstrate that TCEP quenching can be used for super-resolution imaging as well as for other applications, such as differentiating between molecules inside and outside the cell.

Modern biological fluorescence microscopy increasingly relies upon the ability to modulate fluorophores between bright and dark states in order to isolate specific signals of interest. The strategies range widely, including the use of "sensor" fluorophores which selectively react with a given analyte,[1−3] photoswitchable or photactivatable fluorophores for single-molecule-based super-resolution fluorescence imaging,[4−6] contrast enhancement strategies achieved by switching on a desired signal above a constant background fluorescence,[7,8] or fluorescence dequenching as a reporter of vesicle fusion.[9,10] As such, specific modulators of fluorophore properties enable powerful experimental designs. We report here that the red-absorbing dye Cy5 and its structural relatives are reversibly quenched by the water-soluble phosphine tris(2-carboxyethyl)phosphine (TCEP), and we demonstrate the use of the TCEP quenching reaction in super-resolution fluorescence imaging and in a fluorescence internalization assay that can unambiguously differentiate between molecules inside or outside of a cell.

TCEP is a widely used reducing agent for the reduction of disulfide bonds on proteins or small molecules.[11] In the course of preparing a protein sample for labeling with Cy5, we discovered that millimolar concentrations of TCEP strongly quenched the absorption of Cy5. To characterize the spectral properties of the quenching reaction, we incubated Cy5 with various concentrations of TCEP and recorded absorption spectra after the system had reached steady state. The main absorption band of Cy5 at ∼645 nm decreased upon addition of TCEP, and a new band appeared at ∼350 nm (Figure 1A). Quantitative analysis of the quenching as a function TCEP concentration revealed that the quenching behavior is consistent with a reversible bimolecular reaction model with an equilibrium constant of K_{eq} = 0.91 mM^{-1} (Figure 1B). Addition of an excess of the disulfide cystamine to a solution of Cy5 that had already been quenched by TCEP fully dequenched Cy5, corroborating the reversibility of the reaction (Figure S1).

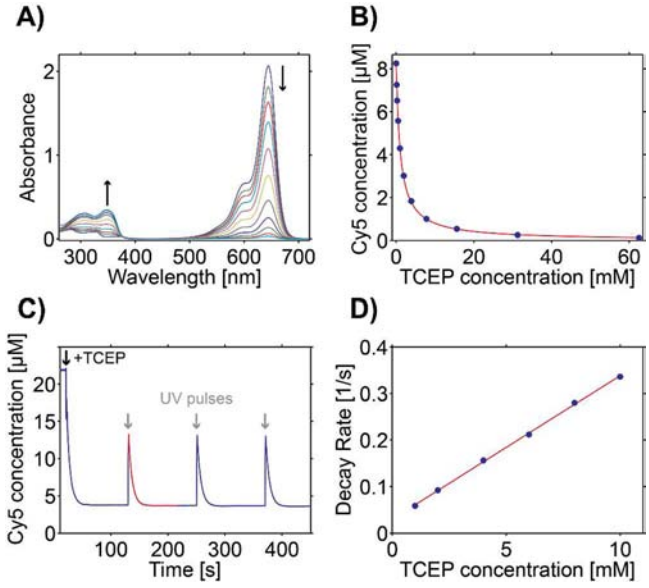

Figure 1. Reversible quenching of Cy5 by TCEP. (A) Absorption spectrum of Cy5 incubated with various concentrations of TCEP, showing a decrease in absorption at ∼645 nm and an increase in absorption at ∼350 nm. (B) Concentration of unquenched Cy5 from (A) as a function of TCEP concentration (blue circles). The red line indicates a nonlinear least-squares fit to the data using the equation $[Cy5] = [Cy5]_0/(K_{eq}[TCEP] + 1)$ with K_{eq} = 0.91 mM^{-1}, which describes a reversible bimolecular reaction between Cy5 and TCEP. (C) Photoreversible quenching of Cy5 by TCEP. At time ∼20 s, TCEP is added to a final concentration of 4 mM, after which 1 s pulses of UV light (centered at 350 nm; gray arrows) transiently reverse the quenching (unquenched Cy5 concentration shown in blue). (D) Decay transients can be fit with an exponential function (red line, (C)) with a rate constant that depends linearly on TCEP concentration, as expected for a reversible bimolecular reaction where $[TCEP] \gg [Cy5]_0$.

Received: October 25, 2012
Published: January 11, 2013

   dx.doi.org/10.1021/ja3105279 | J. Am. Chem. Soc. 2013, 135, 1197−1200

By use of an UV lamp, we found that a solution of TCEP-quenched Cy5 can regain its initial, unquenched blue color, while interrupting the illumination allowed the solution to requench over a period of seconds. The dequenching and requenching process could be repeated many times. Systematic measurements subsequently revealed a linear dependence of the decay rate on TCEP concentration (Figure 1C,D). For a simple, reversible bimolecular reaction where one reactant (TCEP) is much higher in concentration than the other (Cy5, which is <1/50th the concentration of TCEP), the overall decay rate k_{decay} is expected to follow the equation $k_{decay} = k_{off}[TCEP] + k_{on}$, where k_{off} is the rate of quenching and k_{on} is the rate of spontaneous dequenching. From a line-fit of this equation to the measured decay rates, the quenching and dequenching rates were determined to be k_{off} = 0.031 $mM^{-1}sec^{-1}$ and k_{on} = 0.03 s^{-1}, respectively, where the ratio $k_{off}/k_{on} \approx 1.0\ mM^{-1}$ is in good agreement with the steady-state measurement of the equilibrium constant (K_{eq} = 0.91 mM^{-1}; Figure 1B).

We next sought to determine the mechanism of quenching. High-resolution mass spectrometric analysis revealed the presence of an adduct between Cy5 and TCEP ($[M + 4H + Na]^+$ $|m/z|$ observed = 843.2351; expected = 843.2357). Previous work established that Cy5 is able to form an adduct with thiols upon illumination with red light.[12] Because the Cy5-thiol adduct is photogenerated, it was difficult to generate sufficiently large amounts of the Cy5-thiol adduct for analysis by NMR due to the high optical density of solutions containing sufficient Cy5.[12] The Cy5-TCEP adduct, however, forms spontaneously upon mixing, without the need of illumination. It is thus feasible to generate a sufficient amount of the reaction product for analysis by NMR to unambiguously determine the structure of the reaction product.

Initial ^{1}H NMR measurements of Cy5 incubated with fully deuterated TCEP (dTCEP) in D_2O produced congested spectra with overlapping peaks that were difficult to interpret (Figure S2). Fortuitously, we discovered that the terminal protons of the polymethine bridge of Cy5 (H_β and $H_{\beta'}$ in Scheme 1) are exchangeable under acidic conditions, such that

Scheme 1. Formation and Structure of Cy5-TCEP Adduct

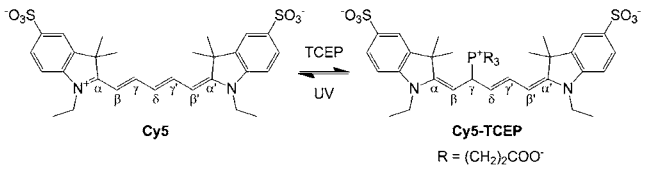

incubation of Cy5 in D_2O for 3 days at pD ~4.5 fully exchanged the terminal bridge protons for deuterons (Figures S3, S4). Incubation of dideuterio Cy5 with dTCEP in D_2O, then, yielded a tractable ^{1}H NMR spectrum (Figures 2 and S5). The γ, γ', δ protons of the polymethine bridge each exhibited doublet of doublet of doublet patterns consisting of eight narrowly resolved peaks, indicating coupling of each proton to the other two nearby protons as well as coupling to the ^{31}P atom of TCEP. Analysis of the coupling patterns revealed the presence of two-, three-, and four-bond phosphorus−hydrogen coupling, establishing that addition of TCEP occurred at the γ-carbon (Scheme 1, Figures 2 and S5). Had TCEP addition occurred at the α-carbon of dideuterio Cy5, no two- or three-bond phosphorus−hydrogen couplings would be observable. Addition of TCEP at the β- or δ-carbons is not expected due to

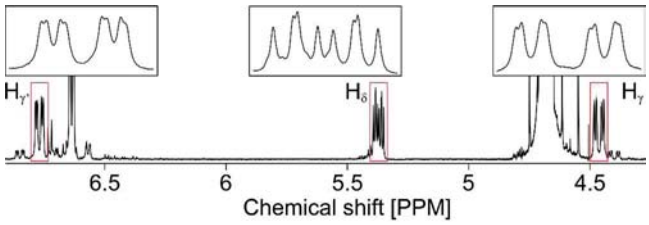

Figure 2. ^{1}H NMR spectrum at 21 °C (600 MHz, D_2O) of the polymethine bridge protons for the dideuterio Cy5-dTCEP adduct. Two-, three-, and four-bond phosphorus−hydrogen coupling was observed in the doublet of doublet of doublet patterns, establishing that TCEP binds at the γ-carbon on Cy5 (see Scheme 1). Note that the large peak at ~4.7 ppm was due to residual water (HOD) and that spinning sidebands are observed on either side of the water peak. See Figure S5 for the full spectrum.

charge conservation considerations[12] and is also not consistent with the NMR spectral data. Taken together, the various lines of evidence indicated a mechanism of quenching consisting of 1,4-addition of TCEP at the γ-carbon of the polymethine bridge of Cy5.

Other carbocyanine dyes were also found to be reversibly quenched by TCEP, including Alexa 647, Alexa 750, and IRdye 800cw, although the carbocyanine dye Cy3 was not quenched (Figure S6). The oxacyanine dye Cy2 was slowly quenched by incubation with TCEP, but the process did not appear to be reversible and may indicate degradation of the dye (Figure S6). Other yellow- or red-absorbing dyes, including rhodamine B, the carboypyronine dye Atto 647N, and the benzopyrillium hemicyanine dye Dyomics 654 also showed little quenching when incubated with TCEP (Figure S6).

Mechanistically, the spontaneous addition of TCEP to Cy5 forms an interesting counterpoint to the photoinduced addition of thiols to Cy5[12−14] now widely used in super-resolution imaging.[4,15−17] Both reactions occur less readily in buffers with pH below the pK_a values of the thiol[12] or phosphine (Figure S7), since the thiolate anion and phosphine lone pair of electrons are required for the reactions. The structure of the TCEP-Cy5 adduct determined by NMR supports our previous proposal that the thiolate anion binds to the γ-carbon of the polymethine bridge of Cy5.[12] In contrast, hard nucleophiles, such as the cyanide anion, have been reported to add to the α-carbon of a nonsulfonated version of Cy5.[18]

While general purpose fluorescence imaging applications may at first seem best served by avoiding fluorescence quenching, many experiments are enabled precisely because of the quenching behavior. As a first application, we show that TCEP-based quenching of cyanines enabled super-resolution imaging by stochastic optical reconstruction microscopy (STORM).[4]

The basic principle of STORM[4] is that individual fluorescent probes are activated and localized with high precision in a sequential manner in order to build up a high-resolution map of the ensemble of probes within the sample. The process relies upon the ability to prepare the majority of molecules in a nonfluorescent state and thereby allow detection of no more than one molecule within any given diffraction limited region at any instant. Critical metrics for evaluating the performance of fluorophores in STORM include the on−off duty cycle, or the fraction of time a fluorophore spends in an "on" (fluorescent) state, and the number of photons detected per fluorophore per activation event.[16] Generally, a low duty cycle is desired, since

the maximum localizable density of fluorescent molecules is roughly inversely proportional to the duty cycle. At the same time, a high number of photons per switching event is desired, since the uncertainty for localizing each molecule scales roughly as the inverse square root of the number of detected photons.

By adding TCEP to an imaging buffer which would otherwise minimize blinking (e.g., a buffer containing an enzymatic oxygen scavenging system and high concentrations of ascorbic acid (AA) and methyl viologen (MV) that are designed to minimize blinking behavior),[19] we observed reversible switching of individual dye molecules when illuminated with ~650 nm light. These switching events were suitable for high-quality STORM imaging (Figure S8). Depending on the concentration of TCEP and the illumination intensity, a range of duty cycles (0.04−0.00013) and detected photons per switching event (1000−4000) could be observed (Figures S9, S10). A TCEP concentration of ~25 mM provided a low duty cycle (0.00013) while maintaining good photons per localization (~2400) and excellent image quality (Figures S8, S10). For imaging experiments, we utilized the structurally similar dye Alexa 647, which showed similar switching behavior to Cy5 in the presence of TCEP (Figure S6).

Although reversible reduction/oxidation reactions using relatively low concentrations of AA and MV can induce switching of Alexa 647[20] and Atto 655,[21] with ~100−400 detected photons per switching event and a duty cycle of ≥0.01, here, TCEP was the primary switching agent. The use of AA and MV, here at relatively high concentrations, minimized transient blinking and bleaching effects[19] and improved the photons per localization. Indeed, when AA and MV were omitted from the imaging buffer, good STORM images were still obtained, although the photons per localization were ~2-fold lower than when all components were used together (Figure S10). On the other hand, omitting TCEP from the buffer strongly degraded the image quality (Figure S10) due to inefficient conversion to a recoverable dark state.

Under the illumination intensities used for imaging (~20 kW/cm^2), the TCEP-Cy5/Alexa 647 photoswitching system gave a comparable number of photons per switching cycle to that of the widely used thiol-Cy5/Alexa 647 system but exhibited a substantially lower duty cycle. The low duty cycle allows more localizations per diffraction-limited area and hence an effectively higher image resolution for densely labeled structures. Moreover, a near-infrared cyanine dye, Alexa 750, emitted far more photons per switching cycle with the TCEP switching system (~2800 detected photons per switching event, Figure S11) than any reported dye in the same spectral range did when thiol is used as the switching agent (<1000 detected photons per switching event).[16] This high photon yield was achieved for Alexa 750 while also maintaining a good duty cycle (0.0003, Figure S12). Based on these properties, the TCEP-based system with Alexa 647 and Alexa 750 is a particularly attractive option for two-color super-resolution imaging (Figure 3).

It is noteworthy that the duty cycle achieved for Cy5/Alexa 647 with 25 mM TCEP under illumination conditions used for STORM imaging (Figures S9, S12) was much lower than would be expected based on the ensemble steady-state and kinetics measurements (Figures 1 and S6). This apparent contradiction may be explained by observing that the duty cycle and off-rate are strong functions of illumination intensity (Figures S9, S12). Whereas the ensemble measurements in Figures 1 and S6 were performed at negligibly low illumination

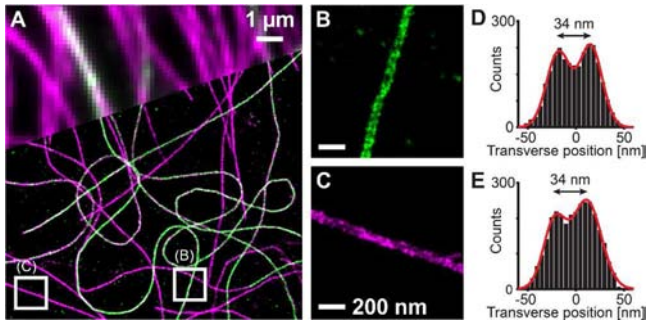

Figure 3. Two-color STORM image of immunolabeled microtubules in a BS-C-1 cell. (A) Tyrosinated tubulin was stained with Alexa 647 (magenta) and detyrosinated tubulin was stained with Alexa 750 (green). (B,C) Single-channel zoom-in images from the boxed regions in (A) both illustrate the hollow structure of the immunolabeled microtubules. The transverse profiles (D,E) correspond to (B,C), respectively, and show double-peak distributions with the expected ~35 nm separation between peaks. The red curves show fits to the distributions by two Gaussian functions.

intensities (~10 mW/cm^2 or lower), the STORM imaging measurements were performed at relatively high illumination intensities (~20 kW/cm^2). The off-rate determined from the ensemble measurements with ~10 mW/cm^2 illumination is much lower than that determined under the STORM illumination intensities but dramatically higher than that expected for a single light-dependent pathway to the dark state, where the off-rate constant scales linearly with light intensity. On this basis, we propose that there are two pathways for dark state formation, one light-independent and one light-dependent and that both contribute to the overall behavior. Upon mixing, a large portion of the fluorophores were quenched due to spontaneous, light-independent formation of the TCEP-dye adduct. Illumination of the sample with ~650 nm light then switched off more dyes and pushed the equilibrium to a lower duty cycle value. It is unclear whether or not the light-independent and light-dependent pathways resulted in the same dark forms.

In a second application, we used TCEP quenching of cyanines as the basis for an internalization assay that can detect whether cargos are outside or inside cells by exploiting the inability of TCEP to cross biological membranes.[22] The basic premise of the assay is that addition of TCEP to the extracellular medium will selectively quench dye molecules bound to cargo outside the cell, while dye molecules bound to internalized cargo will remain fluorescent. This provides a means for assessing whether various fluorescently labeled cargos, such as viruses, proteins, or other dye-labeled structures, have been internalized into the cell, a question commonly encountered when studying endocytosis.

Using the iron-transporting protein transferrin as a model cargo system, we found that the fluorescence from surface-bound cargo was quenched by TCEP, while internalized cargo was not. A549 cells were incubated with Alexa 647-labeled transferrin for 30 min on ice to allow binding but inhibit internalization. Cells were then warmed to 37 °C for various times to allow internalization, followed by fixation (without permeabilization). In cells fixed immediately after binding of Alexa 647-transferrin, nearly all fluorescent punctae were surface associated and quenched when TCEP was added to the imaging medium (Figure 4A). In cells warmed to 37 °C for 15 min prior to fixation to allow near-complete internalization,

dx.doi.org/10.1021/ja3105279 | J. Am. Chem. Soc. 2013, 135, 1197−1200

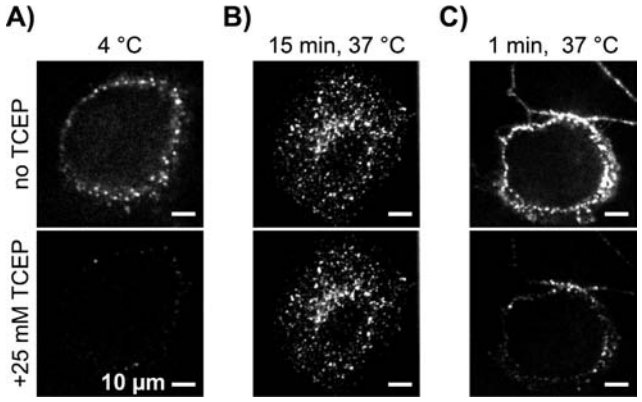

Figure 4. Internalization of Alexa 647-labeled transferrin in A549 cells measured by confocal microscopy. (A) Surface-bound transferrin was quenched upon addition of TCEP to the imaging medium, but (B) internalized transferrin was not. For conditions which allowed partial internalization prior to fixation, (C) some punctae were observed to be internalized, while others are not. Pairs of images are displayed with the same image contrast. 10 μm scale bars.

fluorescent punctae were not quenched by TCEP (Figure 4B). For cells which had been warmed to 37 °C for 1 min prior to fixation, where only a fraction of transferrin was internalized by the cell, a subset of punctae were observed to quench upon addition of TCEP (Figure 4C). Similar experiments using another model cargo, cholera toxin B, also showed similar results (Figure S13).

Evaluation of internalization by TCEP-quenching of cyanine dyes offers some advantages or complementary capabilities compared to previously established internalization assays in that the TCEP-quenching method is reversible, rapid, and makes use of bright fluorophores which are already highly popular for fluorescence imaging applications. A potential disadvantage of the TCEP system is that fluorophores tend to bleach more rapidly when illuminated in the presence of TCEP, although the effect is manageable for applications (Figure S13). The use of moderate to high concentrations of TCEP may also be a potential concern for live-cell internalization studies. However, we found that cells treated with 25 mM TCEP for up to ~6 min showed no obvious morphological changes and that extended treatment up to 15 min did not substantially perturb subsequent cell growth and division in fresh culture medium (data not shown). Since the internalization assay may be completed relatively quickly (≤1 min), this TCEP-based procedure could potentially be used in live cells.

We present here a new tool for on−off modulation of cyanine fluorophores using phosphine-based chemistry. The phosphine TCEP reacts with cyanine dyes spontaneously to form a nonfluorescent adduct by conjugation to the γ-carbon on the polymethine bridge of cyanine dyes. This adduct can be photodissociated to recover the fluorescent state of the dye. TCEP-induced photoreversible quenching allows high-quality super-resolution imaging and an easy-to-implement cellular internalization assay. While we focus on the use of TCEP to quench red- or near-infrared cyanine dyes, other fluorophores quenchable by TCEP may also be found which could potentially extend the utility of the quenching reaction into the blue-green spectral range. Similarly, exploration of other phosphines may improve upon the existing quenching properties as well as expand the palette of probes that can be used for this system.

■ ASSOCIATED CONTENT

Supporting Information

Experimental procedures and Figures S1−S13, including characterization data and STORM images. This material is available free of charge via the Internet at http://pubs.acs.org.

■ AUTHOR INFORMATION

Corresponding Author

zhuang@chemistry.harvard.edu

Notes

The authors declare no competing financial interest.

■ ACKNOWLEDGMENTS

We thank Robert Yu and Shaw Huang for help during this project. This work is in part supported by the NIH. J.C.V. is supported in part by a Burroughs-Wellcome Career Award at the Scientific Interface. E.S. is supported by a NSF graduate research fellowship. X.Z. is a Howard Hughes Medical Institute investigator.

■ REFERENCES

(1) Tour, O.; Adams, S. R.; Kerr, R. A.; Meijer, R. M.; Sejnowski, T. J.; Tsien, R. W.; Tsien, R. Y. *Nat. Chem. Biol.* **2007**, *3*, 423.
(2) Que, E. L.; Domaille, D. W.; Chang, C. J. *Chem. Rev.* **2008**, *108*, 4328.
(3) Ueno, T.; Nagano, T. *Nat. Methods* **2011**, *8*, 642.
(4) Rust, M. J.; Bates, M.; Zhuang, X. *Nat. Methods* **2006**, *3*, 793.
(5) Betzig, E.; Patterson, G. H.; Sougrat, R.; Lindwasser, O. W.; Olenych, S.; Bonifacino, J. S.; Davidson, M. W.; Lippincott-Schwartz, J.; Hess, H. F. *Science* **2006**, *313*, 1642.
(6) Hess, S. T.; Girirajan, T. P. K.; Mason, M. D. *Biophys. J.* **2006**, *91*, 4258.
(7) Marriott, G.; Mao, S.; Sakata, T.; Ran, J.; Jackson, D. K.; Petchprayoon, C.; Gomez, T. J.; Warp, E.; Tulyathan, O.; Aaron, H. L.; Isacoff, E. Y.; Yan, Y. L. *Proc. Natl. Acad. Sci. U.S.A.* **2008**, *105*, 17789.
(8) Richards, C. I.; Hsiang, J. C.; Dickson, R. M. *J. Phys. Chem. B* **2010**, *114*, 660.
(9) Hoekstra, D.; Deboer, T.; Klappe, K.; Wilschut, J. *Biochemistry* **1984**, *23*, 5675.
(10) Lakadamyali, M.; Rust, M. J.; Babcock, H. P.; Zhuang, X. *Proc. Natl. Acad. Sci. U.S.A.* **2003**, *100*, 9280.
(11) Hermanson, G. T. *Bioconjugate techniques*; Thermo Fisher Scientific: Rockford, IL, 2008.
(12) Dempsey, G. T.; Bates, M.; Kowtoniuk, W. E.; Liu, D. R.; Tsien, R. Y.; Zhuang, X. *J. Am. Chem. Soc.* **2009**, *131*, 18192.
(13) Bates, M.; Blosser, T. R.; Zhuang, X. *Phys. Rev. Lett.* **2005**, *94*, 108101.
(14) Heilemann, M.; Margeat, E.; Kasper, R.; Sauer, M.; Tinnefeld, P. *J. Am. Chem. Soc.* **2005**, *127*, 3801.
(15) Heilemann, M.; van de Linde, S.; Schuttpelz, M.; Kasper, R.; Seefeldt, B.; Mukherjee, A.; Tinnefeld, P.; Sauer, M. *Angew. Chem., Int. Ed.* **2008**, *47*, 6172.
(16) Dempsey, G. T.; Vaughan, J. C.; Chen, K. H.; Bates, M.; Zhuang, X. *Nat. Methods* **2011**, *8*, 1027.
(17) van de Linde, S.; Loschberger, A.; Klein, T.; Heidbreder, M.; Wolter, S.; Heilemann, M.; Sauer, M. *Nat. Protoc.* **2011**, *6*, 991.
(18) Niu, H. T.; Jiang, X. L.; He, J. Q.; Cheng, J. P. *Tetrahedron Lett.* **2009**, *50*, 6668.
(19) Vogelsang, J.; Kasper, R.; Steinhauer, C.; Person, B.; Heilemann, M.; Sauer, M.; Tinnefeld, P. *Angew. Chem., Int. Ed.* **2008**, *47*, 5465.
(20) Steinhauer, C.; Forthmann, C.; Vogelsang, J.; Tinnefeld, P. *J. Am. Chem. Soc.* **2008**, *130*, 16840.
(21) Vogelsang, J.; Cordes, T.; Forthmann, C.; Steinhauer, C.; Tinnefeld, P. *Proc. Natl. Acad. Sci. U.S.A.* **2009**, *106*, 8107.
(22) Cline, D. J.; Redding, S. E.; Brohawn, S. G.; Psathas, J. N.; Schneider, J. P.; Thorpe, C. *Biochemistry* **2004**, *43*, 15195.